Highly Efficient Spectrally Encoded Imaging Using a 45° Tilted Fiber Grating

GUOQING WANG,[1] CHAO WANG,[1,*] ZHIJUN YAN,[2,3] LIN ZHANG[2]

[1]*School of Engineering and Digital Arts, University of Kent, Canterbury, CT2 7NT, United Kingdom*
[2]*Aston Institute of Photonic Technologies, Aston University, Birmingham, B4 7ET, United Kingdom*
[3]*State Key Laboratory of Transient Optics and Photonics, Xi'an Institute of Optics and Precision Mechanics, Chinese Academy of Sciences, Xi'an 710119, China*
**Corresponding author: C.Wang@kent.ac.uk*

Received XX Month XXXX; revised XX Month, XXXX; accepted XX Month XXXX; posted XX Month XXXX (Doc. ID XXXXX); published XX Month XXXX

A novel highly efficient, fiber-compatible spectrally encoded imaging (SEI) system using a 45° tilted fiber grating (TFG) is proposed and experimentally demonstrated for the first time. The TFG serves as an in-fiber lateral diffraction element, eliminating the need for bulky and lossy free-space diffraction gratings in conventional SEI systems. Under proper polarization control, due to the strong tilted reflection, the 45° TFG offers a diffraction efficiency as high as 93.5%. Our new design significantly reduces the volume of the SEI system, improves energy efficiency and system stability. As a proof-of-principle experiment, spectrally encoded imaging of a customer-designed sample (9.6 mm × 3.0 mm) using the TFG-based system is demonstrated. The lateral resolution of the SEI system is measured to be 42 µm in our experiment.

OCIS codes: *(050.1950) Diffraction gratings; (110.22970) Image detection systems; (060.3735) Fiber Bragg gratings.*

http://dx.doi.org/10.1364/OL.99.099999

Spectrally encoded imaging (SEI) is a new type of imaging technology, which maps transverse spatial coordinates of the object into wavelength of the illuminating light [1]. The unique one-to-one mapping between space and wavelength is achieved by using diffractive optical elements, such as a diffraction grating for 1D imaging [2] and the joint use of a virtually imaged phased array (VIPA) and a diffraction grating for 2D imaging [3]. SEI technique has attracted considerable research interests due to its features of wide options of illumination wavelength beyond visible light [4], and a great number of resolvable points [5]. However, one difficulty associated with the SEI approach is the poor temporal resolution, which is mainly due to the limited speed in wavelength tuning or spectrum measurement. Recently, a new optical imaging scheme known as serial time-encoded amplified microscopy (STEAM) has enabled ultrafast SEI with unprecedented imaging speed of tens of MHz [3]. This is made possible by adopting a second one-to-one mapping from spectrum to a serial temporal data stream using chromatic dispersion with high-speed single-pixel detection. STEAM technology has been successfully applied in ultrafast laser scanning [6] and flowing particle screening [7], showing great potential in real-time high-throughput measurements [8].

A key element in both SEI and STEAM imaging systems is the diffractive optical device, which encodes the spatial information (image) into the optical spectrum. Diffraction gratings with high groove density are most commonly used due to their high angular dispersion. However, free-space diffraction gratings are usually costly and bulky, which makes miniaturization of SEI systems a real challenge. Most importantly, ruled or holographic diffraction gratings have limited diffraction efficiency (up to 75%) due to the inherent strong zeroth-order reflection. This problem becomes more severe if multiple gratings are used or the diffraction grating also collects light for imaging [3-8]. In STEAM system, in particular, the need for both diffraction gratings and optical fibers to achieve space-to-wavelength mapping and wavelength-to-time mapping, respectively, also results in complex and lossy light coupling between fiber links and free-space optical components. These technical issues hinder widespread application of SEI and STEAM imaging techniques in real practice where low-cost, energy efficient and compact imaging devices are desired.

In this Letter, we propose and experimentally demonstrate a novel highly efficient, fiber-compatible SEI system. Here a 45° tilted fiber grating (TFG) is presented as a highly efficient, compact in-fiber lateral diffractive element in the SEI system, eliminating the need for bulky and lossy free-space diffraction gratings in conventional SEI systems [3-8]. The experimental results indicate that the TFG has a significantly enhanced diffraction efficiency of 93.5%. Moreover, the TFG-based in-fiber diffraction scheme is more desirable in STEAM systems, as the TFG is inherently compatible with optical fibers that provide chromatic dispersion. Not only diffraction loss, but also coupling loss between free-space and fiber optics links will be greatly reduced. Therefore the TFG enables compact and more energy-efficient SEI and STEAM systems.

A TFG is one type of fiber gratings with special characteristics. Its grating structure is tilted with respect to the fiber axis instead of perpendicular to it, which endows it with unique optical properties in comparison with normal fiber Bragg gratings (FBGs) and long period fiber gratings. The concept of TFG was first proposed by Meltz et al. in 1990 [9], and the mode matching mechanism was analysed in great detail by Erdogan and Sipe [10]. In small angle (<10°) TFGs, the propagated light in the fiber core region will be coupled into both backward-propagating core mode and contra-propagating cladding modes, resulting in multiple resonances at the transmission spectrum. In a large angle (such as 45°) TFG, on the other hand, both types of mode couplings are not supported. The light propagation direction is enormously changed due to the largely titled grating structure, which results in direct lateral diffraction into open space in contrast of axial reflection in FBGs, as shown in Fig. 1. In order to fulfil the phase matching condition of broadband side diffraction from the TFG, the lateral diffraction angle is thus strongly wavelength dependent, which makes the TFG a promising candidate for a compact, in-fiber diffractive element. A large angle TFG is a polarization-dependent device. One unique feature of 45° TFGs is that only s-polarized light can be significantly radiated out of fiber core and p-polarized light has a zero transmission loss, making the polarization dependent loss as high as ~40 dB [11]. This unique characteristics allows us to develop it as a highly efficient diffractive optical fiber element by properly controlling the polarization of the incident light. To ensure a high diffraction efficiency, the input light beam should be linearly polarized. Thanks to their unique optical properties, large angle TFGs have found a wide range of attractive applications including in-fiber polarizers [11, 12], a miniature optical spectrum analyser [13], and low-cost optical coherence tomography [14]. Here we propose and demonstrate, for the first time to our best knowledge, the utility of a 45° TFG in spectrally encoded imaging, leading to greatly enhanced energy efficiency, system stability, compactness, and fiber-compatibility.

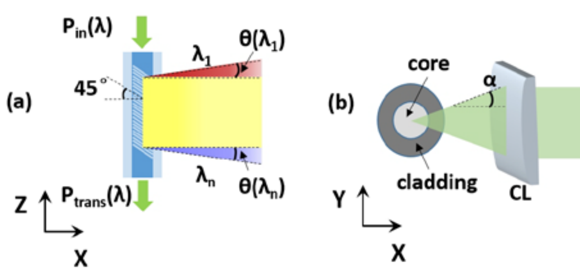

Fig. 1. Principle of a 45° TFG as an in-fiber diffractive element. (a) Wavelength dependent lateral diffraction from the TFG. (b) Divergent output characteristics in radial plane. CL: cylindrical lens.

The structure of a 45° TFG is shown in Fig. 1(a). When the incident light is sent to the TFG, broadband side diffraction is formed due to the largely tilted reflection along the grating structures. Light with different wavelength will be diffracted at different angles. The angular dispersion of the 45° TFG, which characterizes the change of diffraction angle corresponding to a small change in wavelength, is given by [13]

$$D = \frac{d\theta(\lambda)}{d\lambda} = -\sin(2\theta)\frac{1}{\lambda} \tag{1}$$

where λ is the wavelength of incident light, θ is the angle of lateral diffraction. Apparently, a tilt angle of 45° ensures the maximum angular dispersion for a given optical wavelength. For light of 1550 nm, it is thus about 0.037°/nm. Taking the optical refraction at interfaces between fiber core, cladding and air into account, the actual theoretical value of angular dispersion in free space is 0.054°/nm.

Fig. 1(b) illustrates the radial plane view of the lateral diffraction. The emitted light beam is divergent in the radial direction due to the cylindrical shape of the fiber. The divergent angle α is related to the lateral numerical aperture (NA) of the fiber as $NA = \sin(\alpha)$. For imaging purpose, a cylindrical lens is therefore required to collimate the light beam in the vertical (Y-) direction.

A 45° TFG was fabricated to function as an efficient in-fiber diffractive element in the proposed SEI system. The TFG was written directly into a standard telecom single-mode fiber (SMF-28) using the standard scanning phase mask technique with continuous-wave UV-light at 244 nm [15]. To achieve the required 45° slanted grating fringes, the phase mask was rotated by 33.3°. The fabricated TFG is 24 mm long, ensuring high efficiency of diffraction [11].

Performance of the fabricated 45° TFG is first evaluated regarding the specification requirements for SEI. Fig. 2 shows the relation between the diffraction angle and the illuminating wavelength (red dotted black line) within a 30 nm spectral band (1530 – 1560 nm). It is clearly seen that a linear relation (red line) is obtained. The angular dispersion of the 45° TFG is thus estimated to be 0.061°/nm from the measured results, which is in good agreement with theoretically predicted angular dispersion of 0.054°/nm. The discrepancy is mainly due to the measurement error. In addition, the 45° TFG offers a uniform intensity distribution of diffraction with fluctuation less than 0.3 dB across the entire 30nm bandwidth, as shown in Fig. 2. Note that the measured diffraction power was not corrected according to the photodetector's response efficiency, which has a negligible wavelength dependence.

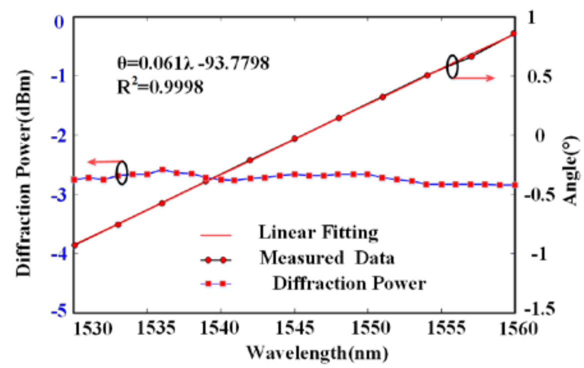

Fig. 2. Measured angular dispersion of the 45° TFG (red-dotted black line) with linear fitting result (red line) and the intensity distribution of lateral diffraction (blue line).

Diffraction efficiency of the fabricated 45° TFG is also measured. As there is no Bragg reflection nor cladding mode coupling in large angle TFGs, when the incident light propagates in the TFG, a portion of it is diffracted into open space while the remaining part keeps propagating in the fiber core. Therefore, diffraction efficiency of the TFG is given by

$$\eta = \frac{P_{diff}(\lambda)}{P_{in}(\lambda)} = \frac{P_{diff}(\lambda)}{P_{diff}(\lambda) + P_{trans}(\lambda)} \tag{2}$$

where $P_{in}(\lambda)$, $P_{diff}(\lambda)$ and $P_{trans}(\lambda)$ are the total input, diffracted and transmitted optical power, respectively. Strength of lateral diffraction from the TFG is largely dependent on the polarization state of the input light with respect to the tilted grating structures [11]. Fig. 3 shows the measured maximum diffraction efficiency at a properly controlled polarization state of the linearly polarized incident light. The average diffraction efficiency of the TFG is as high as 93.5% across the broad wavelength range from 1530 to 1560 nm, which is much higher than that of normal free-space diffraction gratings. This verifies the utility of the 45° TFG as a highly efficient in-fiber diffractive element.

Noting that the diffraction efficiency is also dependent on the length of the TFG [11]. More light can be diffracted by a longer TFG. However, there is an exponential decay in propagation direction for the emitted intensity profile. The diffracted beam pattern from the side of the TFG for a single input wavelength of 1545 nm is measured using a highly-sensitive infrared sensor card and shown in the inset of Fig. 3. It can be seen that our 24-mm long TFG offers strong diffraction while a longer TFG will provide even higher diffraction efficiency.

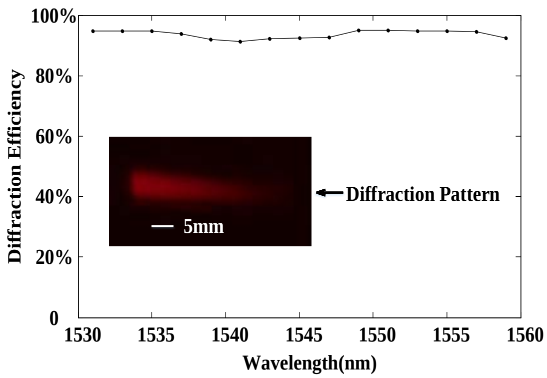

Fig. 3. Measured maximum lateral diffraction efficiency of the 45° TFG at a properly controlled polarization state. Inset: the image of diffraction pattern showing exponential decay.

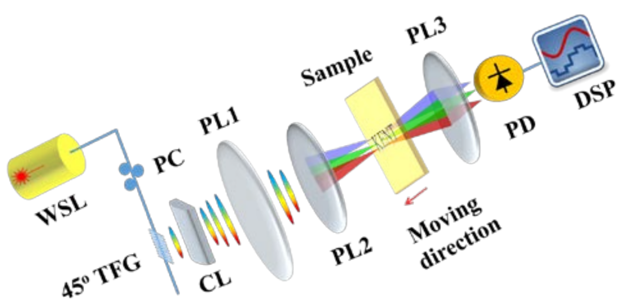

Fig. 4. Schematic diagram of the SEI system based on a 45° TFG. WSL: wavelength swept laser, PC: polarization controller, TFG: tilted fiber grating, CL: cylindrical lens, PL: plain-convex lens, PD: photo-detector, DSP: digital signal processing.

To demonstrate the utility of the 45° TFG in a highly efficient SEI system, we constructed the experimental apparatus as shown in Fig. 4. A wavelength swept laser (Agilent 8168E) was employed to provide broadband illuminating light. The main advantage of using a tunable laser rather than a broadband light source is that here sophisticated optical spectrum analyzer is not required and spectrum measurement can be done using a single-pixel photo-detector in a fast manner. Light from the laser was launched into the fiber containing the 45° TFG, where light was diffracted from one side of the TFG. As the lateral diffraction of light is strongly polarization-dependent, a polarization controller (PC) was employed to maximize the overall diffraction efficiency. The use of 45° TFG as an in-fiber diffraction element significantly reduces the volume of the imaging system as well as the optical insertion loss and the complexity of the system.

A cylindrical lens with a focal length of 20 mm was placed after the TFG for vertical beam collimation. The beam-width of the diffracted light is determined by the length of the TFG (inset, Fig. 3). The diffracted light beams with different wavelengths are largely overlapped in space. To achieve the unique space-to-wavelength mapping for SEI, a lens set is designed to focus different colours of light into separate spatial coordinates on the image plane. The lens set involves two plain-convex lenses with focal lengths of 250 mm and 200mm, respectively, separated by 130 mm.

Our SEI system operates in transmission mode, as shown in Fig. 4, which has the advantages of zero reflection disturbance and low reception loss compared to conventional reflection mode SEI systems. As light can be coupled back from free space to TFG, our system can work in reflection mode as well, which is desired for non-transparent objects. A 2-dimensional (2D) sample with a size of 3.0mm by 9.6mm is used as the test target and placed in the image plane. After the light propagates through the target, the image was encoded onto the spectrum of the illuminating light thanks to the space-to-wavelength mapping. The spectrally encoded light is focused by another plain-convex lens and detected by a single pixel free space photo-detector (PD) with a large active area of 6 mm by 6 mm. Coupling loss from free space to the PD is minimal. The SEI image was finally reconstructed in the digital domain by decoding the spectrally encoded information.

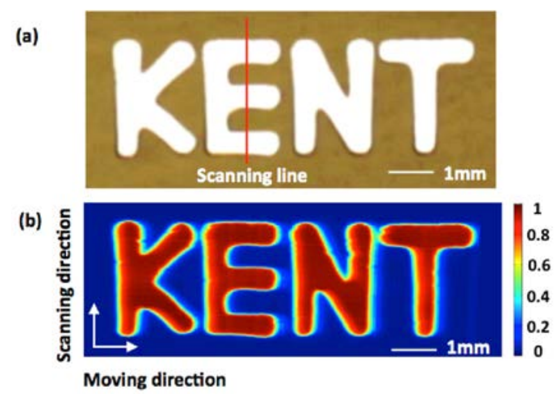

Fig. 5. (a) CCD image of the target with letters "KENT"; (b) the reconstructed dark-field 2D image obtained by the TFG-based SEI system.

The test target is an opaque metal plate with four transparent letters "KENT". The width of strokes in the letters is around 0.6mm. Figure 5(a) shows the CCD image of the customer-designed test target. As a proof-of-concept demonstration, vertical line scanning SEI imaging was carried out by rapidly sweeping the laser wavelength. The step of wavelength scanning is 0.1 nm and the scanning range is 21.5 nm from 1530 to 1551.5 nm. The 2D imaging was achieved by moving the target in the horizontal direction with a step of 30 μm. The reconstructed dark-field 2D image of the target is shown in Fig. 5(b), which clearly shows the word "KENT". The number of pixels in the captured target image is 320×215 (horizontal × vertical). The result firmly verifies the utility of the 45° TFG as an efficient diffractive element in SEI imaging.

Figure 6 shows a vertical line scanning of the right part of letter "E", as shown in Fig. 5(a). Grey shadow areas represent the opaque parts. TFG-enabled one-to-one mapping between the measured optical spectrum and the 1D target appears evident. The reconstructed 1D image matches well with the actual target. Lateral resolution of the TFG-based SEI imaging can be estimated by measuring the point spread function (PSF) of a sharp edge (such as the edges of three horizontal strokes in letter "E"). In our proof-of-concept experiment, lateral resolution of the SEI system is estimated to be 42 μm, as shown in Fig. 6.

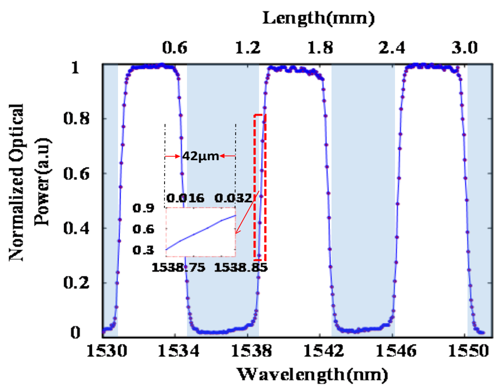

Fig. 6. 1D line scanning image of the right part of letter "E" in the target, obtained by the SEI system. The lateral resolution is estimated to be 42 μm based on the point spread function of a sharp edge.

More study on the spatial resolution of our TFG-based SEI system is conducted with the results shown in Fig. 7. The diffraction-limited spatial resolution is calculated to be 43 μm based on the system parameters. According to the space-to-wavelength mapping relation, the wavelength scanning step of 0.1nm corresponds to a spatial resolution of 14 μm in our system. Point A in Fig. 7 represents the measured resolution in our experiment, which is 42 μm. Therefore, the spatial resolution of our system is diffraction limited. The main aim of this Letter is not to develop high-resolution microscopic imaging, but to demonstrate the first use of a 45° TFG as a highly efficient diffractive element for SEI applications. In fact, the diffraction-limited resolution of our system can be improved by using a high-quality objective lens with shorter focal length and larger numerical aperture.

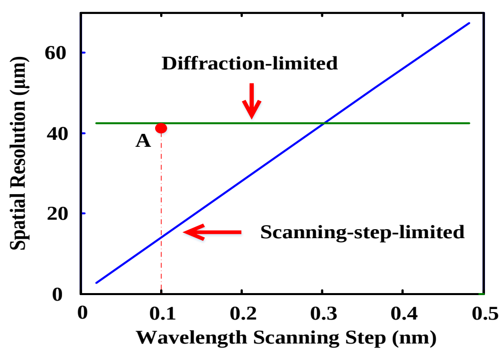

Fig. 7. Spatial resolution of our TFG-based SEI system. The diffraction-limited resolution is calculated as 43 μm (green line) and scanning step limited resolution is shown in blue line. Point A represents the measured system resolution of 42 μm.

The angular dispersion and diffracted beam size are intrinsic for a given 45° TFG. The field-of-view (FOV) and spatial resolution of the imaging system can be adjusted in the free space. For a given lens system, the two parameters are related: higher spatial resolution comes with a smaller FOV. However, the FOV can be further adjusted by changing the spectral bandwidth of the light source.

High-speed realization of SEI, such as STEAM [3], can be implemented by replacing the continuous-wave tunable laser with an ultrafast wavelength-swept light source, which can be made possible by temporally stretching the broadband spectrum of a mode-locked pulsed laser using chromatic dispersion [3]. The imaging speed is then determined by the repetition rate of the pulsed laser, which can be as high as 1 GHz [16]. The TFG is particularly attractive in this ultrafast SEI scheme, as it is inherently compatible with optical fibers or chirped fiber Bragg gratings that provide chromatic dispersion.

In summary, we proposed and experimentally demonstrated a new compact and highly efficient spectrally-encoded imaging system based on a 45° TFG. The TFG served as an in-fiber diffractive element to replace the bulky and lossy free-space diffraction gratings in conventional SEI systems. A 24-mm long 45° TFG was fabricated with its angle dispersion and lateral diffraction efficiency measured to be 0.061°/nm and 93.5%, respectively, across a wide spectral range from 1530 to 1560 nm. As a proof-of-concept demonstration, 2D scanning imaging of a customized target was performed using the TFG-based SEI system. The spatial resolution is measured to be 42 μm, which is diffraction limited. This new design significantly improves the efficiency and reduces the volume, complexity and optical insertion loss of the conventional SEI systems, thus holding great potential in practical applications where portable and low-cost SEI systems are required. In addition, ultrafast SEI can be performed in real-time by adding a time-stretch dispersive Fourier transform configuration. Our technique is particularly promising for ultrafast real-time SEI systems as the TFG disperser is inherently compatible with optical fibers that achieve dispersive Fourier transform.

Funding. EU FP7 Marie Curie Career Integration Grant (631883); Royal Society of UK (RG150036); National Natural Science Foundation of China (61505244).

References

1. D. Kang, B. E. Bouma, and G. J. Tearney, in *Frontiers in Optics* 2011 (Optical Society of America, 2011), p. FML6.
2. G. J. Tearney, M. Shishkov, and B. E. Bouma, Opt. Lett. **27,** 412 (2002).
3. K. Goda, K. K. Tsia, and B. Jalali, Nature, **458**, 1145, (2009).
4. K. Goda and B. Jalali, Nat. Photonics, **7**, 102 (2013).
5. K. Nakagawa, A. Iwasaki, Y. Oishi, R. Horisaki, A. Tsukamoto, A. Nakamura, K. Hirosawa, H. Liao, T. Ushida, K. Goda, F. Kannari and I. Sakuma, Nat. Photonics, **8**, 695, (2014)
6. K. Goda, A. Mahjoubfar, C. Wang, A. Fard, J. Adam, D. R. Gossett, A. Ayazi, E. Sollier, O. Malik, E. Chen, Y. Liu, R. Brown, N. Sarkhosh, D. Di Carlo, and B. Jalali, Sci. Rep. **2**, 445 (2012).
7. K. Goda, A. Ayazi, D. R. Gossett, J. Sadasivam, C. K. Lonappan, E. Sollier, A. M. Fard, S. C. Hur, J. Adam, C. Murray, C. Wang, N. Brackbill, D. Di Carlo, and B. Jalali, PNAS, **109**, 11630 (2012)
8. B. Jalali, D. R. Solli, K. Goda, K. Tsia, and C. Ropers, Eur Phys J-Spec Top., **185**, 145 (2010).
9. G. Meltz, W. W. Morey, and W. H. Glenn, in *Optical Fiber Communication* 1990 (Optical Society of America, 1990), p. TUG1.
10. T. Erdogan, and J. E. Sipe, J. Opt. Soc. Am. A. **13**, 296 (1996).
11. K. Zhou, G. Simpson, X. Chen, L. Zhang, and I. Bennion, Opt. Lett. **30**, 1285 (2005).
12. Z. Yan, C. Mou, K. Zhou, X. Chen, L. Zhang, J. Lightwave Technol. **29**, 2715 (2011).
13. K. Zhou, X. Chen, Z. Yan, A. Adebayo, and L. Zhang, in *Bragg Gratings, Photosensitivity, and Poling in Glass Waveguides* 2012 (Optical Society of America, 2012), p. BW2E.7.
14. S. Remund, A. Bossen, X. Chen, L. Wang, L. Zhang, B. Považay, C. Meier, in *Biophotonics: Photonic Solutions for Better Health Care IV* 2014 (SPIE, 2014), p. 91293G.
15. Y. Zhao, Q. Wang, H. Huang, J. Optoelectron. Adv. M., **12**, 2343 (2010).
16. F. J. Xing, H. W. Chen, M. H. Chen, S. G. Yang, H. C. Yu, and S. Z. Xie, in *Conference on Lasers, and Electro-Optics Pacific Rim (CLEO-PR)* (IEEE, 2013), p. PD1b-2.